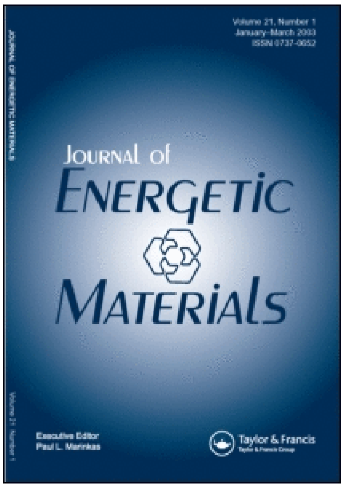

Journal of Energetic Materials
Publication details, including instructions for authors and subscription information:
http://www.informaworld.com/smpp/title~content=t713770432

A refined equation of state for unreacted hexanitrostilbene

Robert E. Setchell[a]; Paul A. Taylor[a]
[a] Sandia National Laboratories, Albuquerque, New Mexico

To cite this Article Setchell, Robert E. and Taylor, Paul A.(1988) 'A refined equation of state for unreacted hexanitrostilbene', Journal of Energetic Materials, 6: 3, 157 — 199

To link to this Article: DOI: 10.1080/07370658808012553

URL: http://dx.doi.org/10.1080/07370658808012553

A REFINED EQUATION OF STATE FOR UNREACTED HEXANITROSTILBENE

Robert E. Setchell and Paul A. Taylor
Sandia National Laboratories
Albuquerque, New Mexico 87185

ABSTRACT

An equation of state for an explosive prior to chemical decomposition is a necessary part of an analytical model for initiation processes. In previous studies of hexanitrostilbene (HNS), a particular equation of state formulation has been used to calculate conditions in shock-compressed material, including temperatures. Measured shock Hugoniot properties were used to find values for parameters appearing in this formulation. In the present study, careful measurements of the isothermal compression of different HNS powders, together with more recent values for thermophysical constants, are used to revise the previous equation of state formulation. Approximate compaction relations for porous HNS are then used to calculate shock Hugoniot states for materials having different initial densities. The predicted states agree closely with available shock Hugoniot data. For shock pressures above 2.5 GPa, the Hugoniot curves predicted in the present study depart progressively from previous predictions.

Journal of Energetic Materials vol. 6, 157-199 (1988)

Published in 1988 by Dowden, Brodman & Devine, Inc.

A reverse-impact experiment was conducted to measure a shocked, unreacted state at a pressure of 8.5 GPa, which is more than twice the highest Hugoniot pressure observed previously. The measured state agrees closely with the revised equation of state formulation. An important consequence of the present study is that predicted shock temperatures are much higher than previous predictions.

INTRODUCTION

An equation of state for an explosive in its unreacted condition is required to establish the thermodynamic states initially produced in the material by a mechanical or thermal stimulus, and to predict the subsequent changes in state properties of the unreacted component once chemical decomposition begins. Thus, an equation of state for the unreacted explosive is an essential part of any analytical model for initiation processes. Direct knowledge of the thermodynamic properties of most condensed explosives, however, is typically restricted to properties measured near ambient conditions and to experimental pressure-compression curves corresponding to isotherms or to the shock Hugoniot.

Hexanitrostilbene (HNS) is a granular explosive, typically pressed without a binder, with good stability under high temperature and vacuum environments.[1] Sheffield et al.[2] measured shock Hugoniot properties at pressures below 4.0 GPa for HNS materials having initial densities from 1.0 to 1.7 g/cm^3 (crystal density is 1.74 g/cm^3). From these measurements and available thermophysical data, they established a particular equation of state for fully shock-compacted (solid), unreacted HNS. Hayes and Mitchell[3] and Hayes[4] used the explicit temperature dependence in this equation of state to examine chemical decomposition of HNS following shock compression. In these studies, the internal energy increase was partitioned between isentropically compressed material and preferentially heated "hot spot" material generated during shock compaction of the initially porous explosive. Relationships were established between initial shock pressures, predicted hot spot temperatures, and hot spot decomposition times inferred from experimental observations. Decomposition times were much shorter than those predicted by a single-step Arrhenius rate law using constants determined at lower temperatures. More recently, hexanitrostilbene has been examined under impact conditions that produce much higher shock pressures.[5] A continuing interest exists in our laboratory to understand the process of shock initiation in this explosive at pressures well above those used in earlier studies, thus prompting a fresh examination of the equation of state formulation.

In the present work, experimental studies of the static compaction of HNS powders have led to a new description for the isothermal compressibility of the solid material. When incorporated into the previous equation of state formulation, along with the most recent measurements of thermophysical properties, significantly different conditions are predicted for shock compression to pressures above 2.5 GPa. The accuracy of the new equation of state is substantiated by the measurement of a shocked, unreacted state at a pressure more than twice that obtained in previous Hugoniot studies.

PREVIOUS EQUATION OF STATE FOR HNS

Sheffield et al.[2] proposed the following specific formulation for the Helmholtz free energy of solid, unreacted HNS:

$$F(T,V) = F(T_o, V_o) + P_o(V_o-V) - S_o(T-T_o) + C_v(T-T_o)[1+\frac{\gamma}{V}(V_o-V)]$$
$$+ C_v T\ln(T_o/T) + \frac{B_{T_o} V_o}{N(N-1)} [(\frac{V}{V_o})^{1-N} - (N-1)(1-V/V_o)-1] , \qquad (1)$$

where T is temperature, V is specific volume, C_v is the specific heat at constant volume, γ is the Grüneisen coefficient, and B_T is the isothermal bulk modulus. A zero subscript identifies ambient conditions. Four assumptions are required in the derivation of this formulation:

(i) The internal energy can be separated into one component which depends on temperature only, and a second component which depends on specific volume only.

(ii) The specific heat at constant volume, C_v, is constant.

(iii) The ratio of the Grüniesen coefficient to specific volume, γ/V, is constant.

(iv) The isothermal compression of solid HNS is described by the compressibility of a Murnaghan solid.

A summary of the derivation of this formulation for the Helmholtz free energy is given in the Appendix. Discussions of the assumptions used in the derivation can be found in Refs. (6-9). Hayes[8] first used equations of state in the form of Eq. (1) to represent the initial and final phases of potassium chloride during shock-induced, polymorphic phase transformations. Johnson et al.[9] used an equation of state in this form to represent the liquid phase in shock-compressed bismuth. Following the initial use of this formulation by Sheffield et al.[2] to represent solid, unreacted HNS, it was used by Hayes[3,4] in subsequent studies of the shock initiation of this explosive.

In order to use Eq. (1) to calculate thermodynamic states, values must be specified for four parameters: the initial isothermal bulk modulus B_{T_o}, the exponent N in the Murnaghan expression for isothermal compressibility (see Appendix), the ratio of the Grüneisen coefficient to specific volume γ/V, and the specific heat at constant volume C_v. Thermophysical properties available to Sheffield et al.[2] consisted of a measured value of the coefficient of linear thermal expansion, and an estimate of the specific heat at constant pressure. Without experimental data on the isothermal compressibility of solid HNS, it was necessary to infer values for the four equation of state parameters from shock Hugoniot data for HNS materials at different initial densities. The procedure they used[10] involves an important assumption. Regardless of the density of the initially porous HNS material, all shock-compressed states are assumed to lie on the Hugoniot curve corresponding to initially solid (non-porous) HNS in the p-V plane. That is, they assumed that an initially porous sample shocked to some specific volume V will have the same pressure as an initially non-porous sample shocked to the same specific volume. With this assumption, Hugoniot data for porous HNS in terms of shock and particle velocities can be plotted in a reduced form so as to represent the corresponding Hugoniot curve for initially solid HNS. A fit to these points then provides the remaining information needed to calculate values for the four parameters in the equation of state. The set of parameter values used in Refs. (2-4) are listed in Table I.

TABLE I. Original Parameter Values for HNS

$B_{T_o} = 14.6$ GPa

$N = 3.465$

$\gamma/V = 2.41$ g/cm^3

$C_v = 1.5 \times 10^7$ cm^2/s^2-K

Very good agreement was obtained between shock Hugoniot conditions predicted with these parameters and the conditions obtained experimentally.

Differences in the p-V shock Hugoniot curves for an initially solid material and for an initially porous sample of the same material have been examined in a number of studies. For example, if a Mie-Grüneisen equation of state is assumed for the porous material, an expression can be derived for the difference in shock pressures between an initially solid material shocked to some specific volume and an initially porous sample of the same material shocked to the same specific volume.[7,11] The shock pressure for the porous material is found to be higher by an amount that depends on the differences in initial densities and on the value of γ/V at the particular specific volume, in agreement with available Hugoniot data for porous aluminum and copper.[7] This result suggests that the procedure used to determine the parameters listed in Table I may have given a non-unique set of values.

ISOTHERMAL COMPRESSIBILITY OF HNS POWDERS

A typical initial density for HNS in current applications is approximately 1.6 g/cm^3, corresponding to a porosity (void volume fraction) of 0.08. During shock initiation, ignition first occurs at discrete hot spots formed by the dynamic shock compression of the porous material. An understanding of this dynamic compaction process is an important element in our goal of developing a predictive model for shock initiation of this explosive. With this purpose in mind, we previously examined the dynamic and static compressibility of various HNS materials having different initial grain size distributions.[12] The static measurements indicated that porosity persisted in the HNS samples up to pressures of at least 6 kbars, but these experiments were not analyzed in any detail. In the present study, these earlier static measurements are carefully re-examined in order to infer the isothermal compressibility of solid HNS.

The static experiments were performed under the conditions of uniaxial strain compression. Starting with loose HNS powders under vacuum, a hydraulic compression system was used to measure how the volume of a given mass of powder varied with applied axial stress at levels up to 2.0 GPa. The compression system consisted of two polished tungsten carbide pistons, 6.35 mm in diameter, closely fitting within a polished, thick-walled (50.0 mm outer diameter), tungsten carbide cylinder. In each experiment, the volume between the pistons was loaded with 400 milligrams of HNS powder, and then evacuated for several hours before starting the compression sequence. The applied axial stress on the powder was determined by carefully measuring the pressure of the hydraulic fluid used to drive one of the pistons. The transmitted axial stress was measured using a stationary load cell in contact with the opposing piston. The relative displacement of the pistons was measured using two LVDT (linear variable differential transformer) displacement instruments. The electrical signals corresponding to applied stress, transmitted stress, and relative piston displacement were converted from analog to digital form and recorded using a small laboratory computer. During a compression experiment, five to ten minutes were allowed of shock temperatures predicted by the present and previous formulations for HNS at an initial density of 1.60 g/cm^3. The possibility of melting has not been considered. At a shock pressure of 10.0 GPa the present formulation gives a temperature of 995 K, which is 230 K higher than previously calculated. Such a difference will have a strong effect on an analytical model of the decomposition chemistry. The temperatures shown in Fig. 11 assume a homogeneous shock-compressed state, and therefore do not reflect the heterogeneous heating that actually occurs in porous HNS due to hot-spot formation processes. However, studies on the shock-initiation properties of very fine-grained HNS indicate that this material behaves very much like a homogeneous explosive over a wide range of initial shock pressures.[25] Hence, for this particular material, temperatures predicted simply with the present equation of state formulation may be quite useful.

ACKNOWLEDGEMENTS

The authors would like to thank Mr. Arni Duncan, Pantex Plant (Amarillo), for providing the HNS powders and their grain size distributions. Mr. Mark Anderson carefully designed and constructed the axial compression apparatus, and Mr. Dave Wackerbarth interfaced its instruments to a laboratory computer for data acquisition and analysis. The reverse-impact experiment to obtain a high-pressure Hugoniot state was skillfully fabricated and conducted by Mrs. Merri Lewis. We would also like to thank Ms. Sharon Healy for her help in preparing the manuscript.

formula for the elastic expansion of a thick-walled cylinder subjected to internal pressure. The value of the constant "a" used in Fig. 1 is within 7% of the value calculated from the cylinder dimensions and the available elastic constants for tungsten carbide. In order for the axial stress to represent the hydrostatic pressure in the sample, the stress must be sufficiently large so that sample shear strength is negligible. The corrected measurements shown in Fig. 1 agree closely with the results from Refs. 13-15 over the range from 0.5 to 1.4 GPa. Above 1.4 GPa there was evidence of increasing friction in the compression fixture, with transmitted stresses dropping progressively relative to applied stresses.

Figure 2 shows the initial grain size distributions for the three HNS powders used in the static compression experiments. Corresponding values of specific surface area are also given. The typical initial grain shape is that of a rod, with the length-to-width ratio increasing from near unity for the smallest grains (HNS-FP) to more than ten for the largest grains (HNS-II). Figure 3 shows the static compression measurements on these powders, corrected for radial expansion of the test fixture, over the axial stress range 0-0.8 GPa. The "Murnaghan fit" shown on this figure will be discussed shortly. The primary experimental uncertainty remaining in these curves is the measurement of powder mass in each case. Sample masses were measured before and after compression tests, with typical differences of 1% occurring due to losses in loading and removing the samples. The mass value used for the HNS-I case was chosen to be the direct average of these two measurements. The mass values used for the other two cases were chosen from within their initial and final measurements so that the resulting densities at 1.0 GPa matched that of HNS-I. The result of this procedure was an extremely close match in densities (to within 0.1%) over the range 0.8 to 2.0 GPa. This result is shown for the entire stress range in Fig. 4. At any given stress below 0.6 GPa, the largest-grained powder, HNS-II, is compressed to a higher density than the intermediate-grained HNS-I, which in turn is compressed to a higher density than the smallest-grained powder, HNS-FP. In a complementary study,[16] we have examined HNS powders recovered from samples previously pressed to stresses from 0.1 to 2.0 GPa. This study has established that grain fracturing is an important compaction mechanism at stresses up to ~ 0.2 GPa for grains having length-to-diameter ratios larger than unity. At higher stresses plastic deformation results in grains that are roughly spherical in shape, with flattened surfaces at boundaries common to adjacent grains.

Above 0.8 GPa, the powder compression curves show no dependence on the initial grain size distribution. At these stresses we expect that shear strength is negligible, and that plastic flow at grain boundaries has reduced porosity to a negligible level. Thus, within the stress range 0.8-2.0 GPa, the axial compression curves can be treated as isothermal compression curves of solid HNS under hydrostatic loading. Consequently, we have fitted the experimental curves in this range with the relation for the isothermal compression of a Murnaghan solid:

$$P-P_o = \frac{B_{T_o}}{N} \left[\left(\frac{V}{V_o}\right)^{-N} - 1 \right] \quad . \qquad (3)$$

The initial isothermal bulk modulus B_{T_o} and the exponent N were chosen so as to minimize the standard deviations from the experimental curves. The result is shown in both Figs. 3 and 4. Above 0.8 GPa, the density predicted by this fit agrees with the experimental curves to within 0.1%.

NEW EQUATION OF STATE PARAMETERS FOR SOLID HNS

The Murnaghan fit to powder compression measurements provides information that was not available to Sheffield et al.[2] when they determined the parameters for their Helmholtz free energy formulation (Table I). In addition to the two new parameters from this Murnaghan fit, an important change has occurred in available thermophysical data. Sheffield et al.[2] used a value of 1.67 x 10^7 cm^2/s^2-K for the specific heat at constant pressure, C_p. The original source for this value[17] identified this number as simply an estimate, with no further elaboration. More recently, several experimental measurements of this specific heat have been reported.[18,19] These independent measurements are in good agreement, and for present purposes we use the most recent value[19] of 1.008 x 10^7 cm^2/s^2-K (at 293 K). The value of γ/V follows from the thermodynamic identities:

$$\frac{\gamma}{V} = \left(\frac{\gamma}{V}\right)_o = \frac{\beta}{C_p} B_{S_o} = \frac{\beta}{C_p} B_{T_o} (1 + \beta\gamma T_o) \ , \qquad (4)$$

where β is the coefficient of volumetric thermal expansion. An experimental value for this coefficient is given in Ref. 18. The initial isentropic bulk modulus B_{S_o} is found from Eq. (4) once γ/V is determined, and the specific heat at constant volume then follows from:

$$C_v = \frac{B_{T_o}}{B_{S_o}} C_p \ . \qquad (5)$$

The resulting set of new parameter values to describe the solid HNS equation of state according to Eq. (1) is given in the following Table:

TABLE II. New Parameter Values for HNS

B_{T_o} = 9.1065 GPa

N = 10.973

γ/V = 2.828 g/cm^3

C_v = 0.889 x $10^7 cm^2/s^2$-K.

The shock Hugoniot relations for initially solid HNS are readily found from Eq. (1). The thermodynamic identities $P = -(\partial F/\partial V)_T$ and $E = F + TS$ are used to find an equivalent equation of state in the form P = P(E,V). The shock jump condition for internal energy,

$$E - E_o = \frac{1}{2}(P+P_o)(V_o-V) \quad , \qquad (6)$$

is used to eliminate internal energy in the P = P(E,V) equation of state, giving an expression which defines the shock Hugoniot curve in the p-V plane. Details of this derivation are given in the Appendix.

EXTENSION TO INTIALLY POROUS HNS

Since HNS materials are pressed from a powder to some density less than crystal density, practical applications of this equation of state necessarily involve initial conditions with finite porosity. In the previous HNS studies using this equation of state,[2-4] all shock-compressed states were assumed to be fully compressed to a non-porous state. The initial specific volume of the porous material was defined to be $\alpha_o V_o$, where V_o remains the reciprocal of crystal density at ambient conditions, and $\alpha_o > 1$. With this notation, the shock jump condition for internal energy becomes:

$$E - E_o = \frac{1}{2}(P+P_o)(\alpha_o V_o-V) \quad . \qquad (7)$$

The derivation of the shock Hugoniot curve in the p-V plane is exactly as before, except that Eq. (7) is used instead of Eq. (6) to eliminate E from the equation of state in the form P = P(E,V).

A more realistic assumption for initially porous material is that finite porosity persists in the shock-compressed state through some range of shock pressures. If the specific volume V is now defined to include any existent porosity, and V_s is defined to be the specific volume of the solid (non-porous) material at the same pressure and temperature, then a convenient measure of porosity is given by:

$$\alpha = V/V_s \tag{8}$$

Finite porosity corresponds to $\alpha > 1$, and α_o is simply the ratio of crystal density to the density of porous material at ambient conditions. Suppose that:

$$P = f(E, V_s) \tag{9}$$

is an equation of state for the solid material at stresses sufficiently high so that shear strength can be neglected. If the specific internal energy of the porous material is assumed to be the same as that of the solid material under identical conditions of pressure and temperature, then Herrmann[20] identified the equation of state for the porous material to be:

$$P = f(E, V/\alpha) \quad , \tag{10}$$

where f is the same function used to describe the solid material. In general, α is a function of the thermodynamic state: $\alpha = \alpha(E,P)$. Along the normal Hugoniot from ambient conditions, however, pressure and internal energy are related. Along this curve, then, we have $\alpha = \alpha(P)$. Herrmann assumed further that this $\alpha = \alpha(P)$ relation will hold in the general vicinity of the Hugoniot curve as well. Thus, if an equation of state in the form of Eq. (9) is available for the solid material, then finding an equation of state in the form of Eq. (10) for the porous material reduces to the determination of the "compaction relation" $\alpha=\alpha(P)$. Herrmann presented a general form of the compaction relation for a ductile, porous material based on its elastic and plastic properties.

Carroll and Holt[21] stated that a better representation of the pressure in the porous material is given by:

$$P = \frac{1}{\alpha} f(E, V/\alpha) \quad . \qquad (11)$$

Assuming only hydrostatic stresses and incompressible, elastic-perfectly plastic material behavior, Carroll and Holt derived a rate-dependent compaction relation. In the plastic regime, the static form of this relation depends only on the material's yield strength. Butcher et al.[22] extended the analysis of Carroll and Holt to include deviatoric stresses and material viscosity, and to account for work hardening during compaction. Good agreement was achieved with both static and shock compaction measurements on porous aluminum.

A careful effort to determine an accurate compaction relation for porous HNS is beyond the scope of the current study. Rather, such an effort will be the nature of our future work. For present purposes, an approximate compaction relation used previously for some porous metals will be utilized in order to illustrate calculations of shock-compressed states in initially porous HNS. Herrmann[20] noted that a simple quadratic form had been adequate for describing shocked states in porous iron. This form is given by:

$$\frac{\alpha-1}{\alpha_e-1} = \left(\frac{P_s-P}{P_s-P_e}\right)^2 , \qquad (12)$$

where P_s is the pressure corresponding to complete void elimination ($\alpha=1$), and the subscript "e" denotes values at the elastic limit. Herrmann also derived an approximate expression for the speed of a weak compaction wave:

$$C_b = \frac{\alpha_e C_o}{(\alpha_e - B_{S_o} \alpha_e')^{1/2}} , \qquad (13)$$

where $C_o = (V_o B_{S_o})^{1/2}$ is the bulk sound speed in the solid, and α_e' is the slope of the $\alpha(P)$ relation at the elastic limit. For an $\alpha(P)$ relation in the form given by Eq. (12):

$$\alpha_e' = \frac{-2(\alpha_e-1)}{P_s-P_e} . \qquad (14)$$

Measurement of the speed of a weak compaction wave gives a value for α_e' through Eq. (13), and Eq. (14) can then be used to find the value of P_s needed to use the $\alpha(P)$ relation given by Eq. (12). In our earlier study of the compaction of HNS powders,[12] planar-impact techniques were used to introduce 1.5 GPa ramp waves (0.6 μs rise times) into HNS samples initially pressed to a density of 1.60 g/cm^3. The observed propagation velocity of the "toe" of these ramp waves was 1.73 ± .03 km/s. Using this measurement as the speed of a weak compaction wave in material at this initial density, together with the parameter values from Table II, allows us to use Eq. (13) to find:

$$\alpha_o' = -0.123 \text{ GPa}^{-1}$$

The elastic strength has been assumed to be negligible in this calculation, so that ambient conditions are used instead of conditions at the elastic limit (i.e., $\alpha_e = \alpha_o$ and $P_e = P_o$). Using this value in Eq. (14), we find: $P_s = 1.43$ GPa. By using this value of P_s in Eq. (12), an approximate compaction relation is defined for HNS at an initial density of 1.60 g/cm^3. This $\alpha(P)$ relation has a reasonable slope near ambient conditions, but whether or not the consequence that $\alpha \rightarrow 1$ as $P \rightarrow 1.43$ GPa is a good approximation under shock-compaction conditions is not yet known.

In order to test this simple compaction relation, shock Hugoniot curves have been calculated for comparisons with available measurements. Because the speed of a weak compaction wave only has been measured at an initial density of 1.60 g/cm^3, a linear variation of this speed with α_o was assumed to hold from the bulk sound speed at $\alpha_o = 1$ (1.74 g/cm^3) through the measured speed at $\alpha_o = 1.0875$ (1.60 g/cm^3). With this assumption, parameters used for the approximate $\alpha(P)$ relation at various initial densities are listed in Table III.

TABLE III. Parameters for Approximate $\alpha(P)$

Initial Density-g/cm^3	C_b - km/s	P_s - GPa
1.71	2.30 (est.)	2.42
1.60	1.73 (meas.)	1.43
1.58	1.62 (est.)	1.26

These three $\alpha(P)$ relations are plotted in Fig. 5.

In calculating shock Hugoniot conditions for initially porous states, the equation of state for solid HNS in the form $P=f(E,V)$ (see Appendix) is rewritten in the form of Eq. (11):

$$P = \frac{1}{\alpha} f(E, V/\alpha)$$

where $\alpha(P)$ is given by Eq. (12) and the parameters in Table III. Internal energy is again eliminated by substituting the shock jump condition as it appears in Eq. (6), with specific volumes corresponding to the porous material. The resulting expression relates P, $\alpha(P)$, and V, and defines the shock Hugoniot curve in the P-V plane. Figure 6 shows the results of numerical calculations of shock Hugoniot states for two different initial densities, together with the available shock Hugoniot data at those densities. Also shown in Fig. 6 are the corresponding shock Hugoniot curves calculated in Ref. 2. The two sets of calculations agree closely over the range of available data, but at higher particle velocities the shock pressures predicted from the present analysis are progressively higher than those predicted in Ref. 2.

HIGH PRESSURE SHOCKED STATE MEASUREMENT

In Fig. 6 the Hugoniot curves calculated in the present study are very close to the original predictions of Sheffield et al.[2] over the stress range of the experiments. The comparisons shown in this figure, therefore, are not conclusive in establishing that more accurate predictions of shock-compressed states are now possible. To address this uncertainty, we conducted a planar impact experiment as shown in Fig. 7. HNS-I pressed to a density of 1.60 g/cm^3 was accelerated to a velocity of 1.33 km/s, then impacted into a Z-cut sapphire target. VISAR instrumentation[23] was used to record the particle velocity history at the impact interface. The shock Hugoniot properties of Z-cut sapphire[24] were then used to find the stress history of the HNS/sapphire interface. The result is shown in Fig. 8. The unusually slow, stepped rise in this stress history is due to a projectile-driven gas shock wave reverberating between the target and projectile faces. This gas shock resulted from poor vacuum ahead of the projectile and/or blow-by of gas from behind the projectile. The relatively slow compression shown in Fig. 8 resulted in a significant delay in the onset of observable chemical reactivity. For sharp-shock loading to the same final stress, extrapolated results from an earlier study by Hayes[4] indicated that a delay of only ~5 ns could be expected. The observed delay was approximately 200 ns, which made the determination of unreacted state properties much easier. The HNS stress-particle velocity state measured in this experiment is shown in Fig. 9, together with Hugoniot curves predicted by the current analysis and as predicted by the original analysis of Sheffield et al.[2] The uncertainty in the measured stress is primarily due to uncertainty in the sapphire Hugoniot curve. The 8.5 GPa stress level in the HNS is more than twice that obtained in previous shock Hugoniot experiments. The accuracy of the present analysis is strongly supported by the agreement shown with the measured state. However, an important consideration is whether the measured state could be displaced from the shock Hugoniot due to a reduction in entropy production resulting from the finite compression rate. As an example of the utility of the equation of state formulation, we can examine this displacement from the shock Hugoniot for the limiting case of an isentropic compression. First, the thermodynamic relation that results from combining the first and second laws, $dE = TdS - PdV$, reduces to:

$$dE = -PdV \qquad (15)$$

for an isentropic process. In the Appendix, Eq. (A15) is an equation of state for solid HNS in the form $P = f(E,V)$. As discussed in the previous section, an equation of state for porous HNS can be written:

$$P = \frac{1}{\alpha} f(E, V/\alpha) \quad ,$$

where $\alpha = \alpha(P)$ is the compaction relation. This can be rewritten in the form:

$$E = E(\alpha P, V/\alpha) \quad , \tag{16}$$

where the pressure dependence includes that introduced by $\alpha(P)$. Differentiating Eq. (16) and combining with Eq. (15):

$$dE = \left(\frac{\partial E}{\partial P}\right)_V dP + \left(\frac{\partial E}{\partial V}\right)_P dV = - PdV \tag{17}$$

Equation (17) is a differential equation for the isentrope in a P-V plane. Once a compaction relation $\alpha(P)$ is specified, this equation can be integrated numerically.

Figure 10 shows a calculated isentrope for HNS at an initial density of 1.60 g/cm^3. The simple quadratic form for $\alpha(P)$ (Fig. 5) was used in this calculation. The predicted Hugoniot curves and the measured state are also shown in the P-V plane for comparison. The specific volume identified with the measured state is the value given by the shock jump conditions under the assumption of steady wave propagation. In reality, the specific volume of this state lies somewhere between the Hugoniot and the isentrope at the measured pressure. At the pressures shown, the calculated isentrope is insensitive to the particular form chosen for $\alpha(P)$. Although an isentropic compression of porous HNS to high densities is not physically realistic, this curve represents a limit to displacements from the shock Hugoniot for adiabatic processes in which entropy production may be reduced. For compressions to a particular pressure, an isentropic process results in a lower specific volume than that produced by a shock wave. At the measured pressure, however, the predicted Hugoniot and isentrope curves are still relatively close to each other, in comparison to the Hugoniot curve predicted by the previous formulation.

CONCLUSIONS

In the present study, we have used careful measurements of isothermal compressibility, together with revised values for thermophysical constants, to improve the equation of state formulation for HNS initially proposed by Sheffield et al.[2] Measurement of a high-pressure shocked state supports the accuracy of the new formulation. Shock Hugoniot curves calculated using the new equation of state parameters lie above the previous calculations at pressures above 2.5 GPa, so that shock pressures generated in HNS under high-velocity impact conditions[5] are significantly higher than previously thought. A major remaining task is the formulation of an appropriate compaction relation $\alpha(P)$ for porous HNS, although very simple approximations give good agreement with available low-pressure shock Hugoniot data.

The use of more recent determinations of specific heat values has a very strong effect on predicted shock temperatures. Because these specific heat measurements have resulted in a much lower value than the estimated value used previously, predicted shock temperatures are much higher. Figure 11 shows a comparison to lapse after an incremental increase in hydraulic fluid pressure before the stresses and relative displacement were measured. The total time for an experiment to 2.0 GPa on a given powder sample was between three and four hours.

In order to make quantitative use of the powder compression data, all possible corrections to account for experimental aberrations needed to be examined. The elastic compression of the tungsten carbide pistons was measured in tests without powder samples up to the maximum stress of 2.0 GPa. Friction due to lateral expansion of the pistons against the cylinder walls was not apparent in these tests. A significant correction was necessary to account for radial expansion of the thick-walled tungsten carbide cylinder enclosing the sample and pistons. In order to determine the necessary correction, compression tests were performed on a reference material whose isothermal compressibility has been extensively studied. Figure 1 shows the results of using single-crystal sodium chloride to determine the required radial expansion correction. The axial stress is the average of the applied and transmitted stresses. The corrected specific volume V at any pressure P is in the form:

$$V = V^1 (1 + P/a)^2 \quad , \qquad (2)$$

where V^1 is the measured volume neglecting radial expansion, and "a" is a constant that depends on the elastic constants and dimensions of the cylinder. Eq. (2) follows from the handbook

This work performed at Sandia National Laboratories was supported by the U. S. Department of Energy under Contract #DE-AC04-76DP00789.

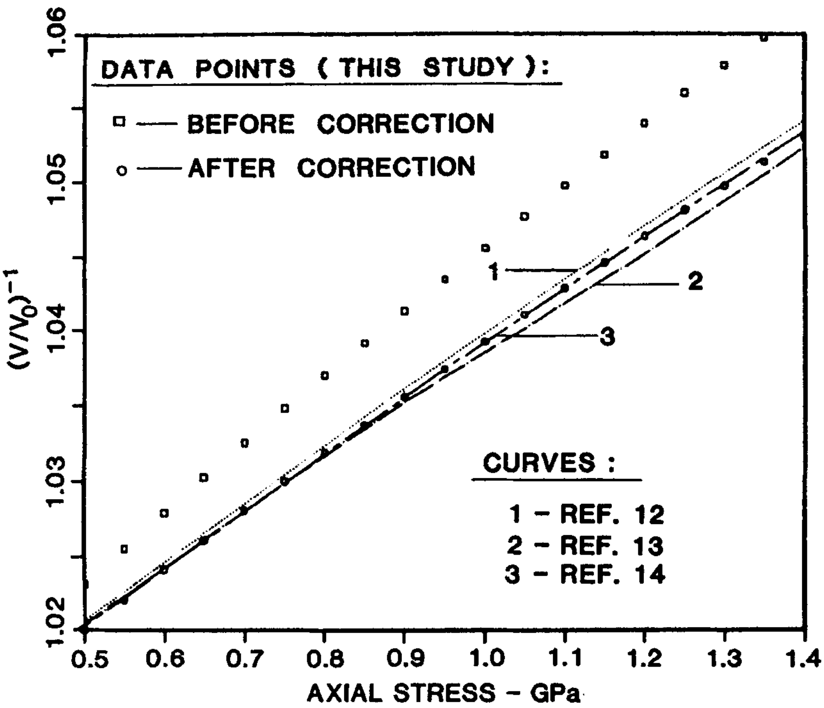

FIGURE 1

Measurement of the isothermal compression of single-crystal sodium chloride. Comparisons with previous studies were used to determine the required correction for radial expansion of the cylinder enclosing the sample and pistons.

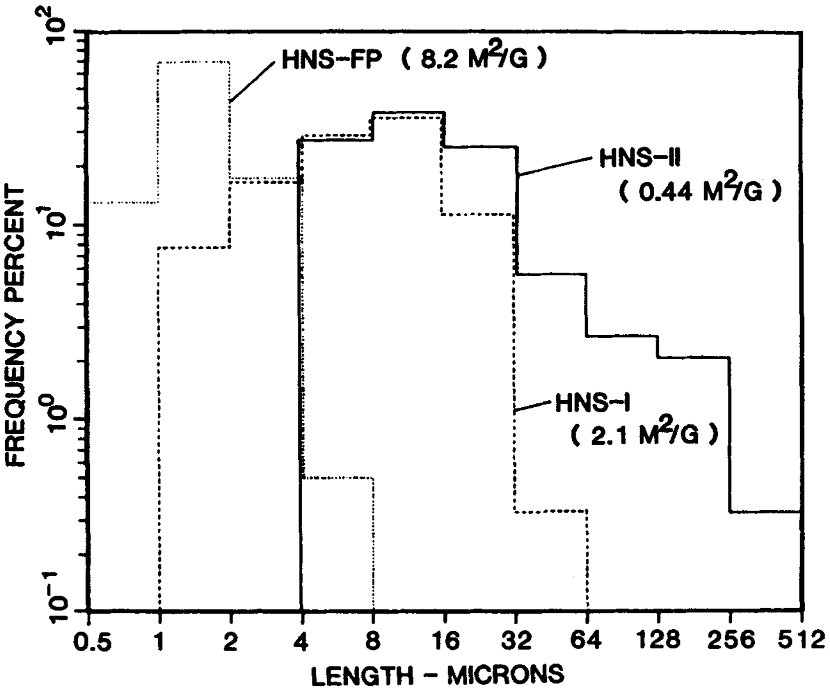

FIGURE 2

Grain size distributions for the three HNS powders used in isothermal compression experiments. The corresponding specific surface areas are also shown.

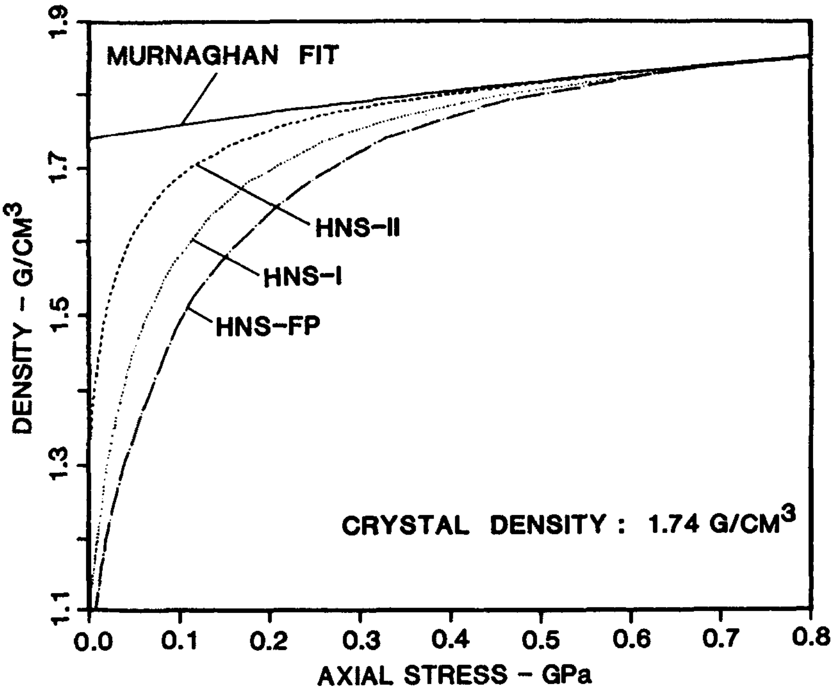

FIGURE 3

Measurements of powder density at average axial stresses up to 0.8 GPa. The Murnaghan curve is a fit to measured densities at higher pressures (Fig. 4).

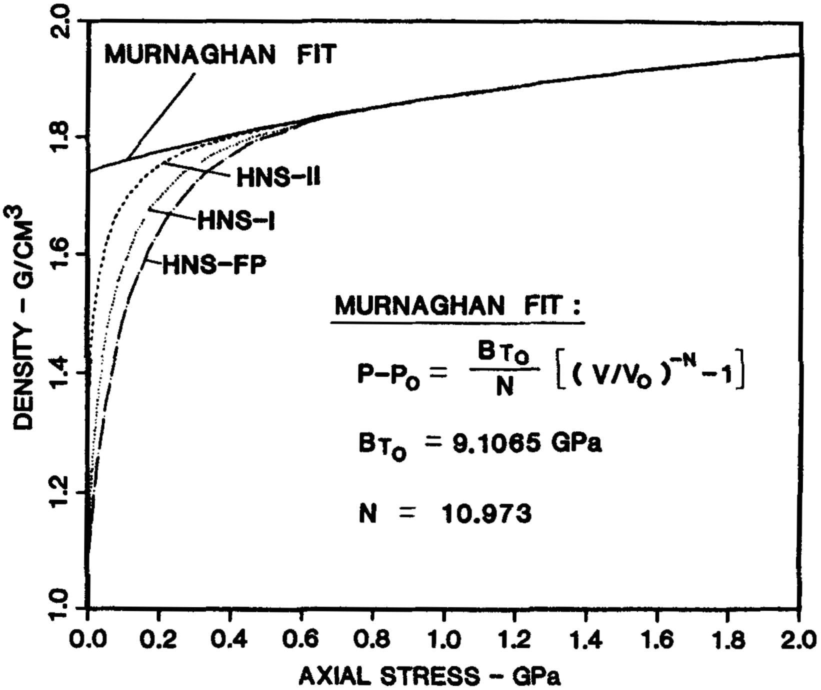

FIGURE 4

Measured powder densities at axial stresses up to 2.0 GPa. The individual powder curves collapse to a single curve at higher pressures, and are closely fit by the expression for isothermal compression of a Murnaghan solid.

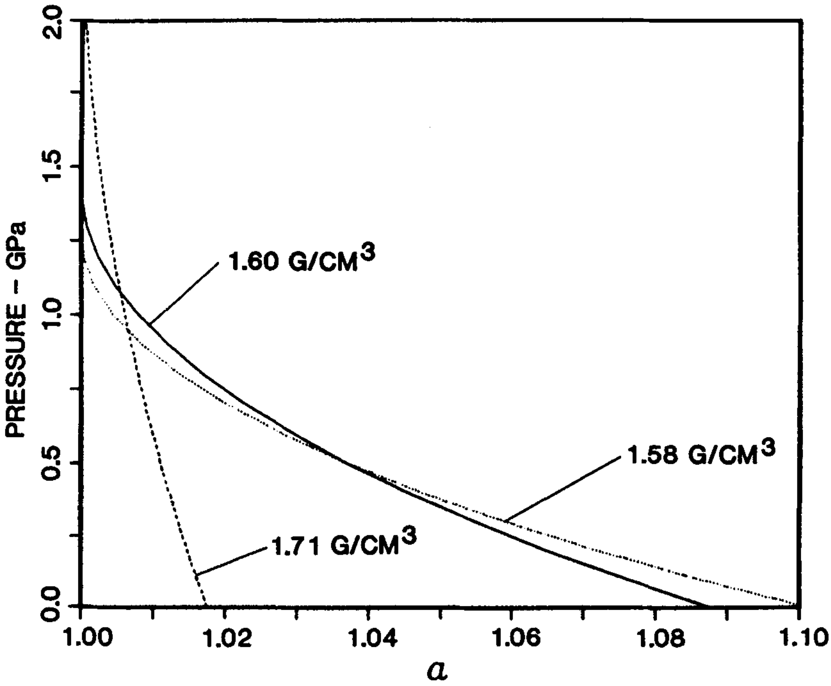

FIGURE 5

Approximate compaction relations $\alpha(P)$ for HNS at different initial porosities.

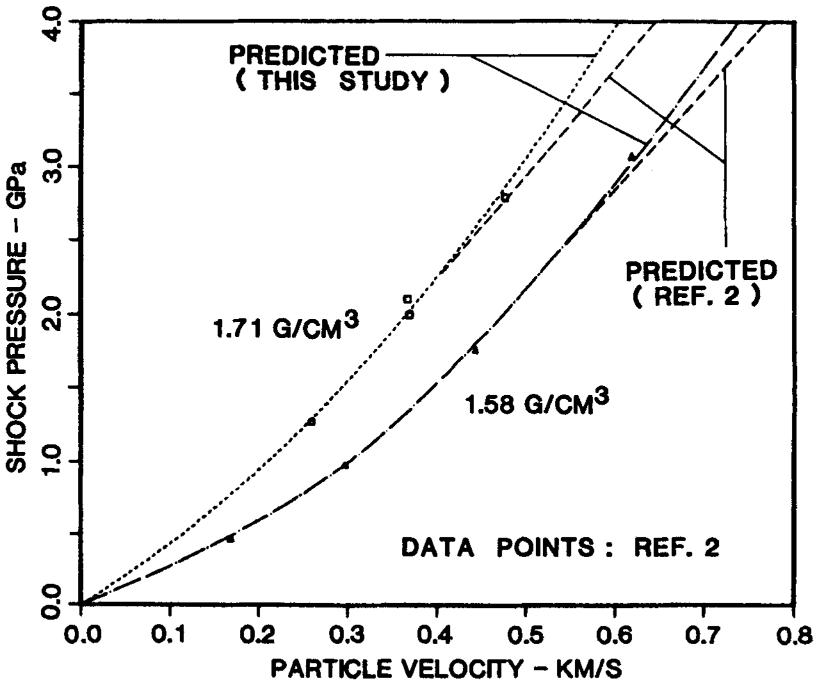

FIGURE 6

Comparisons at two different initial densities between shock Hugoniot data and Hugoniot states predicted using the present equation of state formulation and the approximate compaction relations shown in Fig. 5. Hugoniot states predicted by the previous analysis (Ref. 2) are also shown.

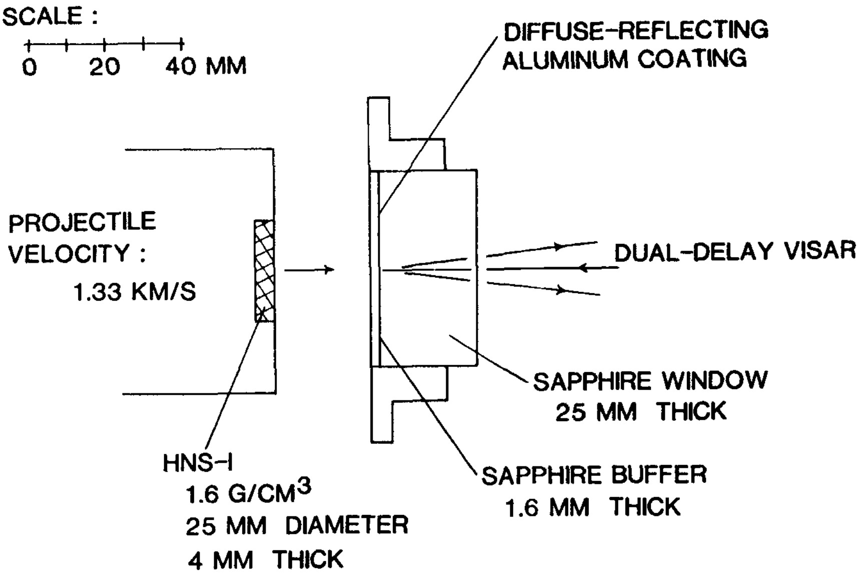

FIGURE 7

The reverse-impact configuration used in a gas gun experiment to measure a high-pressure shock Hugoniot state in HNS having an initial density of 1.60 g/cm^3.

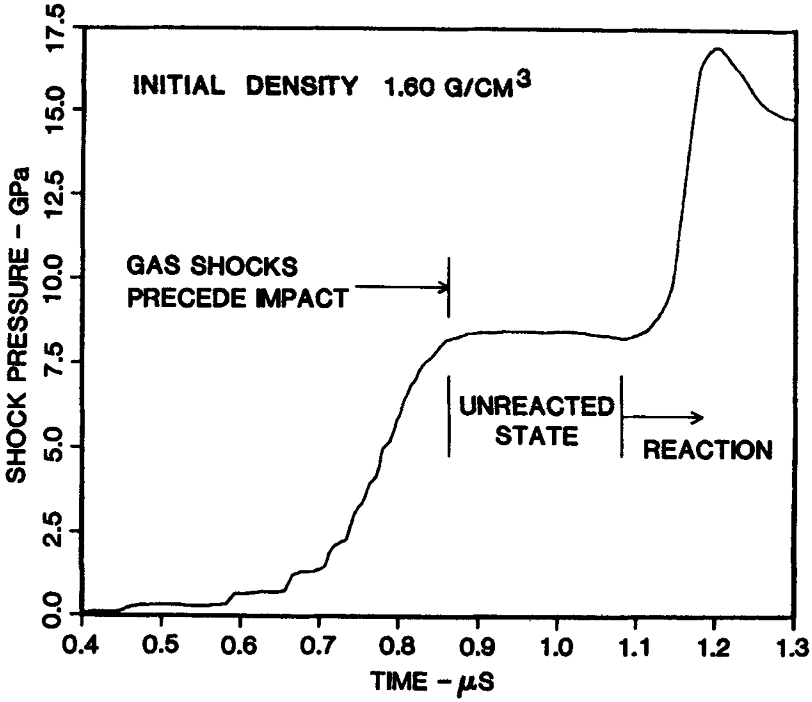

FIGURE 8

The stress history at the HNS/sapphire impact interface obtained in the reverse-impact experiment. The unusually slow rise is due to a strong gas shock reverberating between the projectile and target faces.

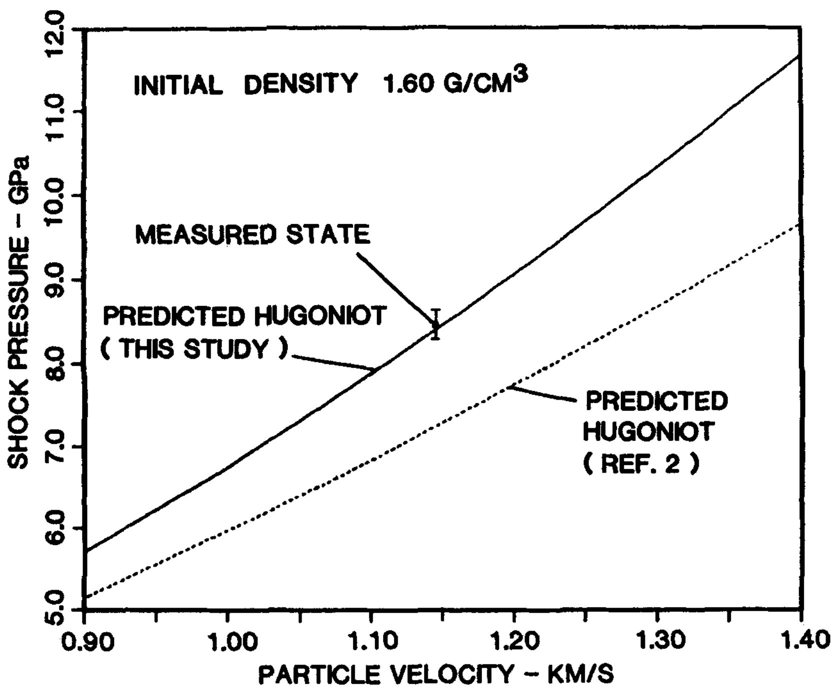

FIGURE 9

Comparisons between the measured high-pressure state in HNS, the Hugoniot states predicted by the current equation of state formulation, and the Hugoniot states predicted by the previous analysis (Ref. 2) for an initial density of 1.60 g/cm^3.

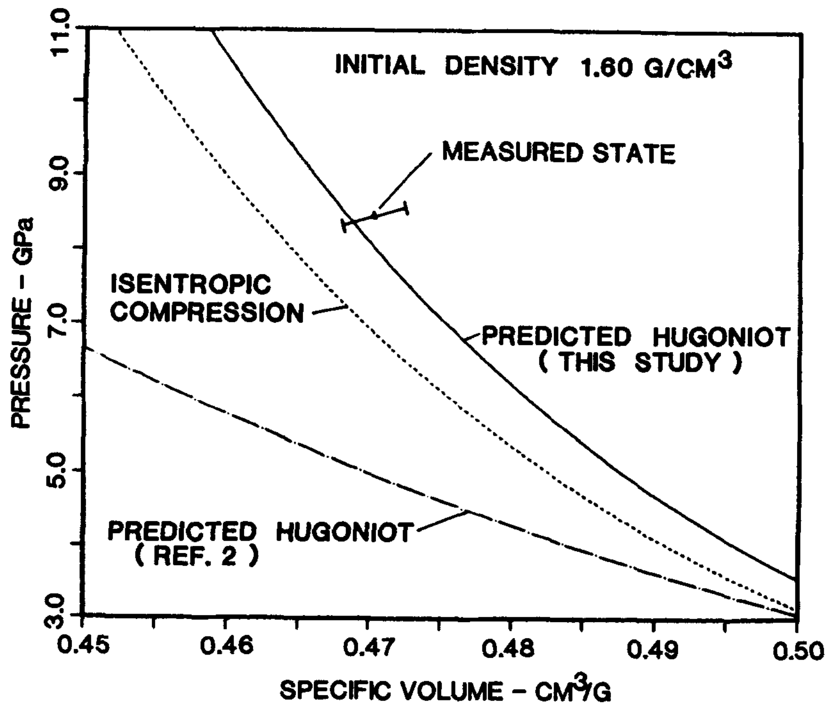

FIGURE 10

Comparisons between the measured state and the predicted Hugoniot curves in the P-V plane, together with an isentropic compression curve calculated using the current equation of state formulation. The specific volume for the measured state was calculated assuming steady wave propagation.

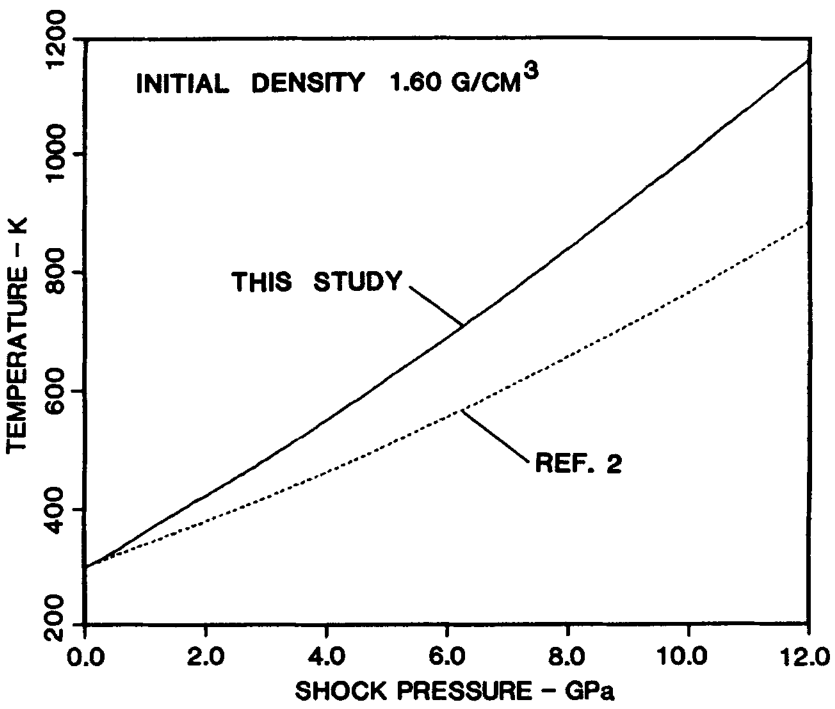

FIGURE 11

Comparisons between the shock temperatures predicted by the present analysis and those predicted by the previous analysis (Ref. 2) for an initial HNS density of 1.60 g/cm^3.

REFERENCES

1. E. E. Kilmer, J. Spacecraft 5, 1216 (1968).
2. S. A. Sheffield, D. E. Mitchell, and D. B. Hayes, in "Proceedings of the Sixth Symposium (International) on Detonation," Office of Naval Research, ACR-221, Arlington, VA, 1976, p. 748.
3. D. B. Hayes and D. E. Mitchell, in "Symposium (International) on High Dynamic Pressures," Commissariat a l'Energie Atomique, Paris, 1978, p. 161.
4. D. B. Hayes, in "Shock Waves, Explosions, and Detonations," J. R. Bowen, N. Manson, A. K. Oppenheim, and R. I. Soloukin, eds., AIAA Progress in Astronautics and Aeronautics Vol. 87, AIAA, New York, 1983, p. 445.
5. A. C. Schwarz, in "Proceedings of the Seventh Symposium (International) on Detonation," Naval Surface Weapons Center, NSWC MP 82-334, White Oak, MD, 1982, p. 1024.
6. M. Cowperthwaite, Am. J. Phys. 34, 1025 (1966).
7. For example, see W. J. Carter, S. P. Marsh, J. N. Fritz, and R. G. McQueen, in "Accurate Characterization of the High-Pressure Environment," E. C. Lloyd, ed., National Bureau of Standards Special Publication 326, Washington, DC, 1971, p. 147.
8. D. B. Hayes, J. Appl. Phys. 45, 1208 (1974).

9. J. N. Johnson, D. B. Hayes, and J. R. Asay, J. Phys. Chem. Solids 35, 501 (1974).

10. D. E. Mitchell, S. A. Sheffield, and D. B. Hayes, Sandia National Laboratories Report SAND76-0109 (1976).

11. J. O. Erkman and D. J. Edwards, in "Proceedings of the Sixth Symposium (International) on Detonation," Office of Naval Research, ACR-221, Arlington, VA, 1976, p. 766.

12. R. E. Setchell and P. A. Taylor, in "Shock Waves in Condensed Matter," Y. M. Gupta, ed., Plenum Press, New York, 1986, p. 871.

13. E. A. Perez-Albuerne and H. G. Drickamer, J. Chem. Phys. 43, 1381 (1965).

14. J. N. Fritz, S. P. Marsh, W. J. Carter, and R. G. McQueen, in "Accurate Characterization of the High-Pressure Environment," E. C. Lloyd, ed., National Bureau of Standards Special Publication 326, Washington, DC, 1971, p. 201.

15. D. L. Decker, J. Appl. Phys. 42, 3239 (1971).

16. P. A. Taylor and R. E. Setchell, to be published.

17. S. Marantz and G. T. Armstrong, J. Chem. Eng. Data 13, 118 (1968).

18. B. M. Dobratz and P. C. Crawford, Lawrence Livermore National Laboratory Report UCRL-52997 Change 2 (1985).

19. E. P. Roth, Sandia National Laboratories, private communication.

20. W. Herrmann, J. Appl. Phys. 40, 2490 (1969).

21. M. M. Carroll and A. C. Holt, J. Appl. Phys. 43, 1626 (1972).

22. B. M. Butcher, M. M. Carroll, and A. C. Holt, J. Appl. Phys. 45, 3864 (1974).

23. For example, see R. E. Setchell, Combust. Flame 54, 171 (1983).

24. R. A. Graham and W. P. Brooks, J. Phys. Chem. Solids 32, 2311 (1971).

25. R. E. Setchell, in "Proceedings of the Eighth Symposium (International) on Detonation," Naval Surface Weapons Center (in press).

APPENDIX: EQUATION OF STATE DERIVATION

The Helmholtz free energy for solid, unreacted HNS proposed by Sheffield et al.[2] is given by:

$$F(T,V) = F(T_o,V_o) + P_o(V_o-V) - S_o(T-T_o) + C_v(T-T_o)[1+\frac{\gamma}{V}(V_o-V)]$$
$$+ C_vT\ln(T_o/T) + \frac{B_{T_o}V_o}{N(N-1)}\,[(\frac{V}{V_o})^{1-N}-(N-1)(1-V/V_o)-1] \quad . \quad (1)$$

To derive this expression, it is first assumed that the internal energy can be separated into two independent components which depend only on temperature and on volume, respectively. As discussed by Cowperthwaite,[6] this initial assumption results in a P-V-T equation of state in the form:

$$P = (\frac{\partial P}{\partial T})_V \cdot T + g(V) \quad , \qquad (A1)$$

where $(\frac{\partial P}{\partial T})_V$ is either a constant or a function of V only, f(V). If C_v is assumed to be constant, which is often assumed for solids above their Debye temperature, the P-V-T equation of state has the general form:

$$P = f(V) \cdot T + g(V) \quad , \qquad (A2)$$

and an E-P-V equation of state has the form:

$$E = [C_v/f(V)]\ P + g_1(V) \qquad (A3)$$

where $C_v/f(V) = (\partial E/\partial P)_V = \frac{V}{\gamma}$, and $g_1(V)$ is a function related to $g(V)$. Eqs. (A2) and (A3) are equivalent to assuming a Mie-Grüneisen equation of state.[6] Using the thermodynamic identity $\frac{\gamma}{V} = (\partial P/\partial T)_V/C_v$, it can be seen that adding the assumption $\frac{\gamma}{V}$ = constant is equivalent to assuming $(\partial P/\partial T)_V$ = constant. This assumption often has been used to determine isentropes and isotherms that neighbor experimentally determined shock Hugoniots.[7] Letting $b = (\partial P/\partial E)_V = \gamma/V$, Eqs. (A2) and (A3) become:

$$P = bC_vT + g(V) \tag{A4}$$

and

$$E = P/b + g_1(V) \tag{A5}$$

The form of the Helmholtz free energy function that corresponds to these expressions is:

$$F(T,V) = C_vT + g(V)/b + g_1(V) - T\{S_o - bV_oC_v(1-V/V_o) + C_v\ln(T/T_o)\} \tag{A6}$$

which can be shown by finding $S = -(\partial F/\partial T)_V$, calculating $E = F + TS$, and comparing with Eqs. (A4, A5). If the isothermal compressibility of solid HNS is assumed to be that of a Murnaghan solid, then it has the form:

$$B_T = -V\left(\frac{\partial P}{\partial V}\right)_T = B_{T_o}\left(\frac{V}{V_o}\right)^{-N}, \tag{A7}$$

where P is hydrostatic pressure. This assumption allows the determination of the functions not yet specified in Eq. (A6). Integrating Eq. (A7) along the $T = T_o$ isotherm gives:

$$P - P_o = \frac{B_{T_o}}{N} \left[\left(\frac{V}{V_o}\right)^{-N} - 1\right] \qquad \text{(A8)}$$

Combining Eqs. (A4) and (A8):

$$g(V) = P_o - C_v b T_o + \frac{B_{T_o}}{N} \left[\left(\frac{V}{V_o}\right)^{-N} - 1\right] \quad . \qquad \text{(A9)}$$

Finally, since $P = C_v bT + g(V) = -(\partial F/\partial V)_T$, we have:

$$dg/dV + bg + b\, dg_1/dV = o \qquad \text{(A10)}$$

Substituting Eq. (A9) into Eq. (A10) and integrating:

$$g_1(V) = E_o - P_o/b + V_o(P_o - bC_v T_o)(1 - V/V_o)$$
$$+ \frac{V_o B_{T_o}}{N} \left(\left[\frac{\left(\frac{V}{V_o}\right)^{1-N} - 1}{N-1}\right] - \left[\frac{\left(\frac{V}{V_o}\right)^{-N} - 1}{bV_o}\right] - (1 - V/V_o) \right) \qquad \text{(A11)}$$

Substituting Eqs. (A9) and (A11) into Eq. (A6) gives the final expression for the Helmholtz function as it appears in Eq. (1).

Equivalent forms of this equation of state can be found easily. First, a P-V-T equation of state is given by:

$$P = -(\partial F/\partial V)_T = P_o + \frac{\gamma}{V} C_v (T - T_o) + \frac{B_{T_o}}{N} \left[\left(\frac{V}{V_o}\right)^{-N} - 1\right]$$

(A12)

An S-T-V equation of state is given by:

$$S = -(\partial F/\partial T)_V = S_o + C_v\,[\ln(T/T_o) - \frac{\gamma}{V}(V_o - V)] \qquad (A13)$$

Internal energy, E = F + TS, is given in the form E(T,V) by:

$$E = E_o + P_o\,(V_o - V) + C_v\,(T - T_o) - \frac{\gamma}{V}\,C_v T_o\,(V_o - V)$$

$$+ \frac{B_{T_o} V_o}{N(N-1)}\,\{(\frac{V}{V_o})^{-N+1} - (N-1)(1 - V/V_o) - 1\} \;. \qquad (A14)$$

To simplify subsequent expressions, let

$$f_1(V) = \frac{\gamma}{V}\,C_v T_o (V_o - V),\quad f_2(V) = \frac{B_{T_o}}{N}\,[(\frac{V}{V_o})^{-N} - 1],$$

$$\text{and } f_3(V) = \frac{B_{T_o} V_o}{N(N-1)}\,\{(\frac{V}{V_o})^{-N+1} - (N-1)(1 - V/V_o) - 1\} \;.$$

Thus, Eq. (A14) can be written:

$$E - E_o = P_o(V_o - V) + C_v(T - T_o) - f_1(V) + f_3(V) \;.$$

Substituting for $C_v(T-T_o)$ in this expression using Eq. (A12):

$$E - E_o = \frac{P - P_o}{(\gamma/V)} + P_o(V_o - V) - f_1(V) - \frac{f_2(V)}{(\gamma/V)} + f_3(V) \;, \qquad (A15)$$

which is an equation of state in the form E = E(P,V) or P = P(E,V).

The shock Hugoniot relation for solid HNS is found by combining Eq. (A15) with the shock jump condition for internal energy, $E - E_o = (1/2)(P + P_o)(V_o - V)$. The result defines the Hugoniot curve in the P-V plane:

$$P - P_o = [\frac{\gamma}{V} f_1(V) + f_2(V) - \frac{\gamma}{V} f_3(V)]/f_4(V) \;, \qquad (A16)$$

where $f_4(V) = 1 - \frac{1}{2}(\frac{\gamma}{V})(V_o - V)$.